A Minkowski Interval Analysis Sensitivity Tool for Analyzing the Impact of Amplifiers Tolerances in Planar Arrays

L. Tenuti, N. Anselmi, P. Rocca, M. Salucci, and A. Massa

Abstract

Due to manufacturing problems or to environmental changes, some deviations can be observed on the nominal value of amplifiers used in the beamforming network of planar arrays. As a consequence, the radiated pattern may differ from the expected one, and the overall system performances can undergo a certain performance degradation. In this document, an interval analysis (IA)-based sensitivity tool is proposed to mathematically derive bounds on the radiated field by planar arrangements starting from the tolerances of the amplifiers of the control points. The developed approach is based on the Minkowski sum, rather than on standard Cartesian arithmetic. Some numerical results are shown, to prove the effectiveness of the Minkowski IA tool in estimating narrower pattern bounds than the standard Cartesian IA.

1 Numerical Assessment - Planar Array - Analysis vs Amplitude Tolerance

GOAL: this section considers the analysis of tolerances on the amplifiers of the control points of planar array with different number of elements, i.e., a 10×5 and a 10×10 planar array. The amplitude tolerances have been increased from the $1\,\%$ to the $5\,\%$ of the nominal value. The objective is to prove that, when tolerances on amplifiers are present the use Cartesian or Minkowski intervals lead to the same results.

Array geometry:

- Uniform planar array: $N \times M = 10 \times 5$, $N \times M = 10 \times 10$
- Inter-element spacing: $d_x = 0.5$ $[\lambda]$ - $d_y = 0.5$ $[\lambda]$.

Nominal control points:

- Separable distributions:
  - x-axis: Dolph-Chebyshev pattern: $SLL = 20$ $[dB]$.
  - y-axis: Dolph-Chebyshev pattern: $SLL = 20$ $[dB]$.

Tolerances on the control points:

- Amplitude tolerance: $\delta\alpha_n = \pm 1\,\%, \pm 3\,\%, \pm 5\,\%$.
- Phase tolerance: $\delta\beta_n = 0$ $[deg]$

Minkowski sum parameters:

- Number of sides including polygon: $L = 720$

1.1 10×5 Array Elements

Nominal Pattern

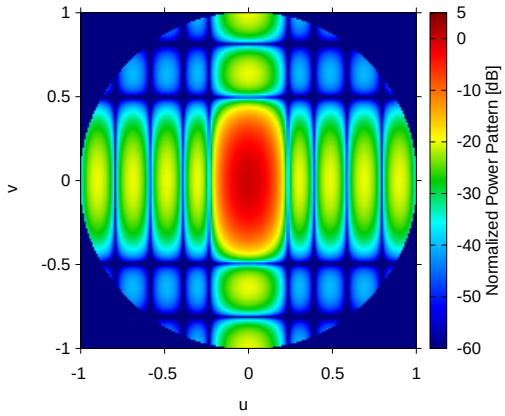

Figure 23

Nominal Pattern Features

$BW\ [v] - u = 0$	$BW\ [u] - v = 0$	$SLL\ [dB] - u = 0$	$SLL\ [dB] - v = 0$	$PP\ [dB]$
0.412	0.196	-20.0	-20.0	29.29

Table VII

1.1.1 Amplitude Error 1 %

Interval Pattern

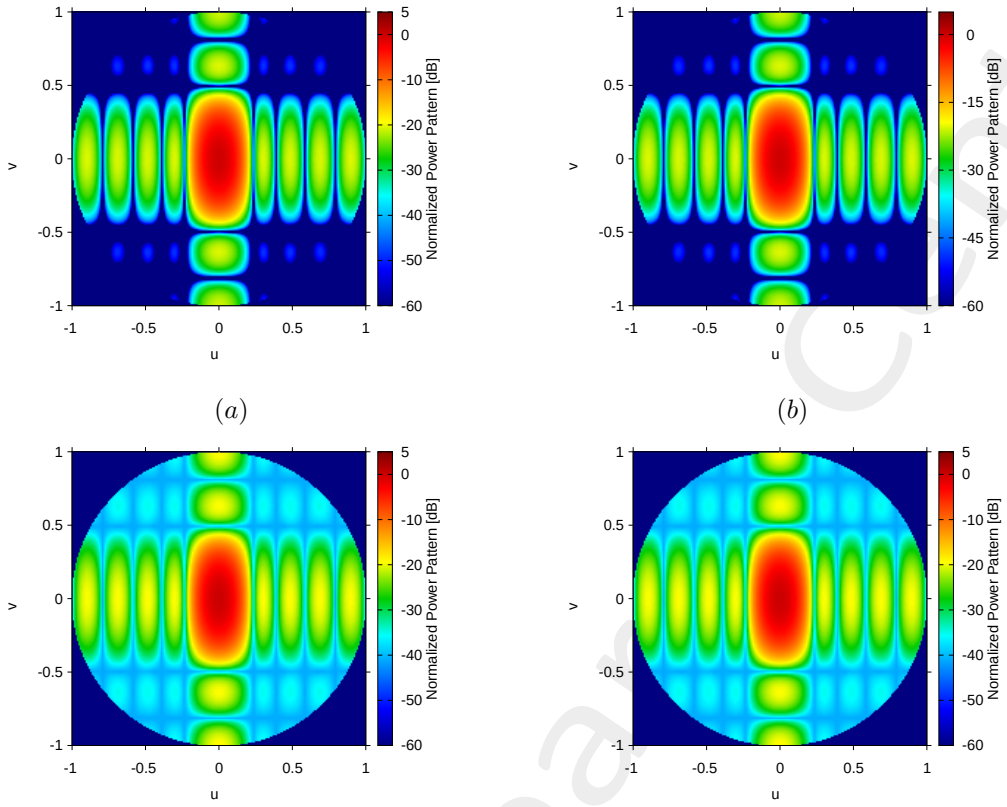

(a) (b)

(c) (d)

Figure 24: Infimum of the power pattern Cartesian (a) and Minkowski sum (b), Supremum of the sum power pattern Cartesian (c) and Minkowski (d) sum

Cuts on the plane $(0, v)$ - $(u, 0)$ - Interval Pattern

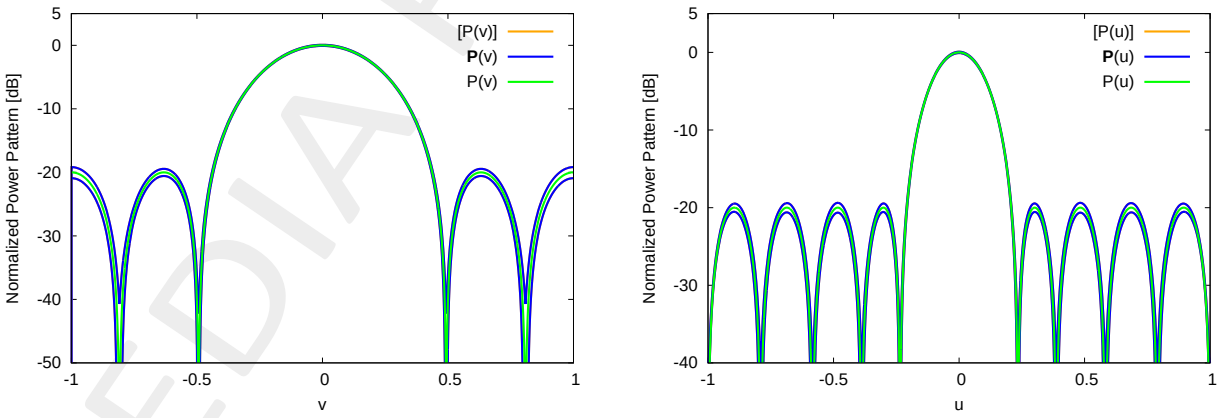

(a) (b)

Figure 25:

1.1.2 Amplitude Error 3 %

Interval Pattern

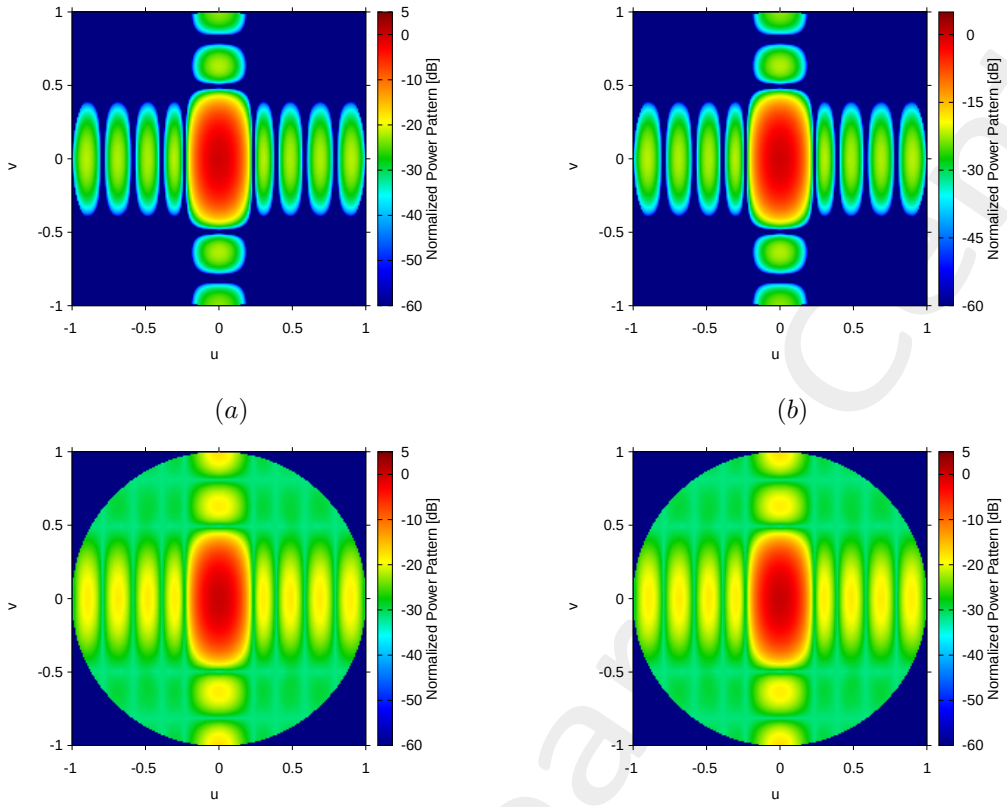

(a) (b)

(c) (d)

Figure 26: Infimum of the power pattern Cartesian (a) and Minkowski sum (b), Supremum of the sum power pattern Cartesian (c) and Minkowski (d) sum

Cuts on the plane $(0, v)$ **-** $(u, 0)$ **- Interval Pattern**

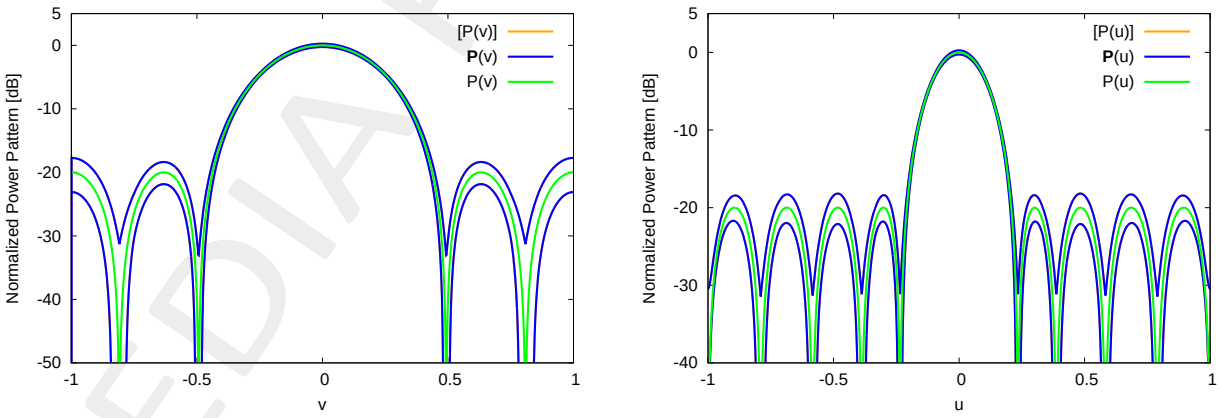

(a) (b)

Figure 27:

1.1.3 Amplitude Error 5 %

Interval Pattern

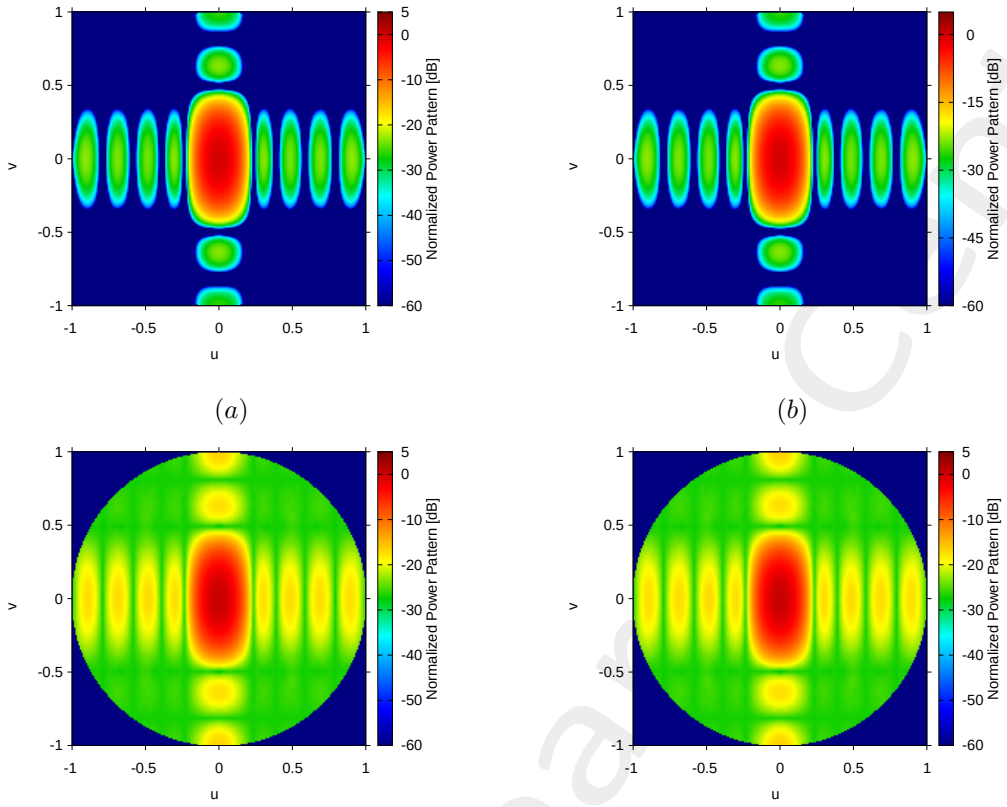

(a) (b)

(c) (d)

Figure 28: Infimum of the power pattern Cartesian (a) and Minkowski sum (b), Supremum of the sum power pattern Cartesian (c) and Minkowski (d) sum

Cuts on the plane $(0, v)$ - $(u, 0)$ - Interval Pattern

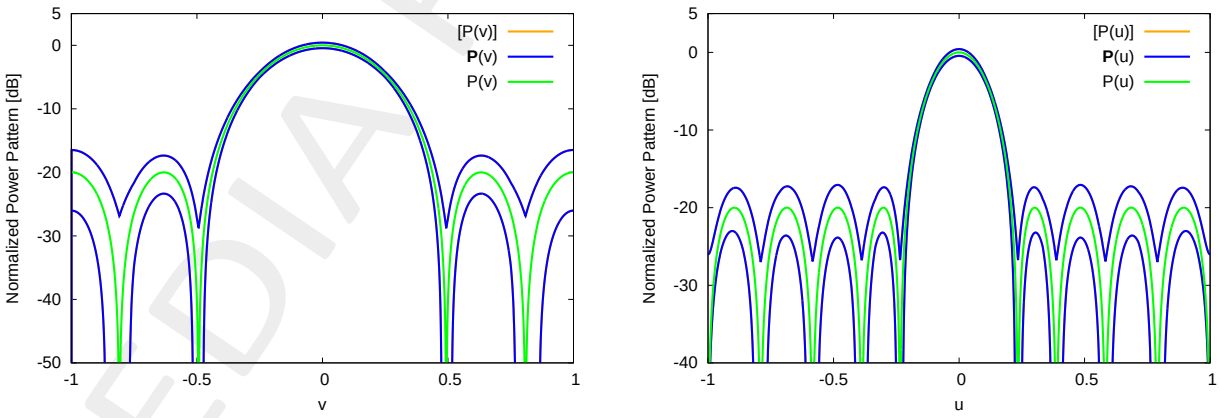

(a) (b)

Figure 29:

1.1.4 Analysis vs Amplitude Tolerance

Pattern

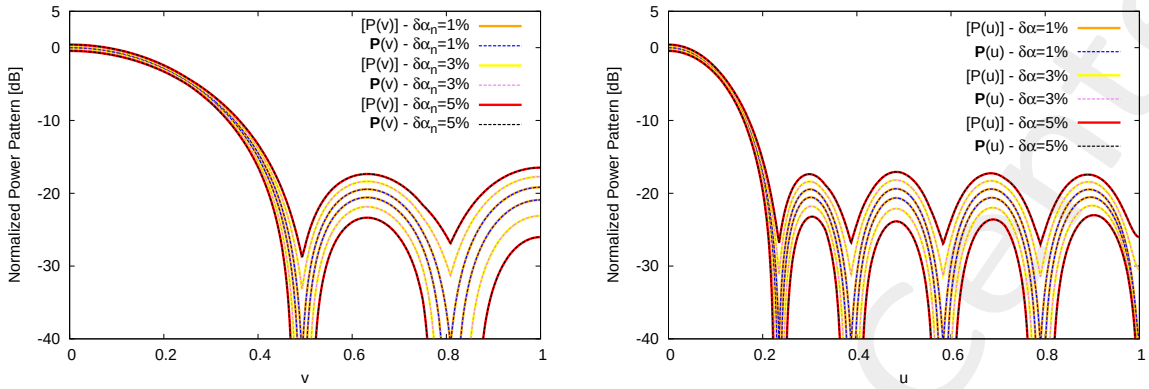

(a) (b)

Figure 30:

Interval Beamwidth

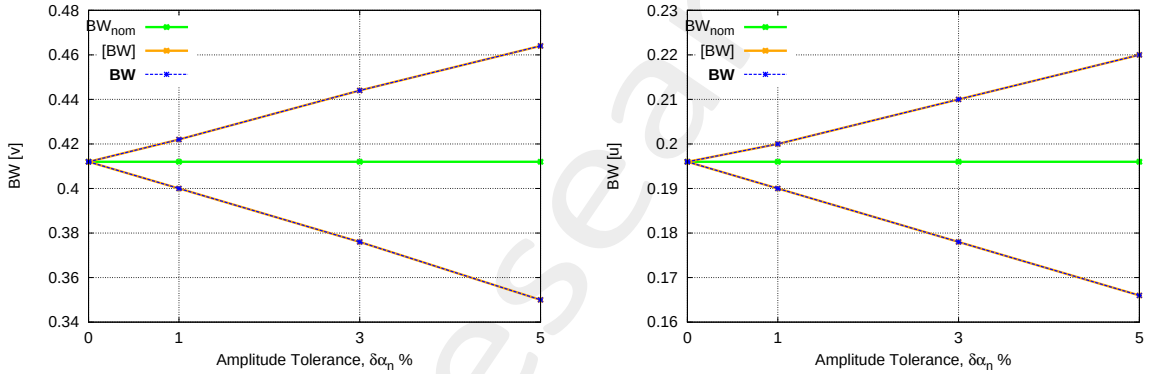

(a) (b)

Figure 31:

Interval SLL

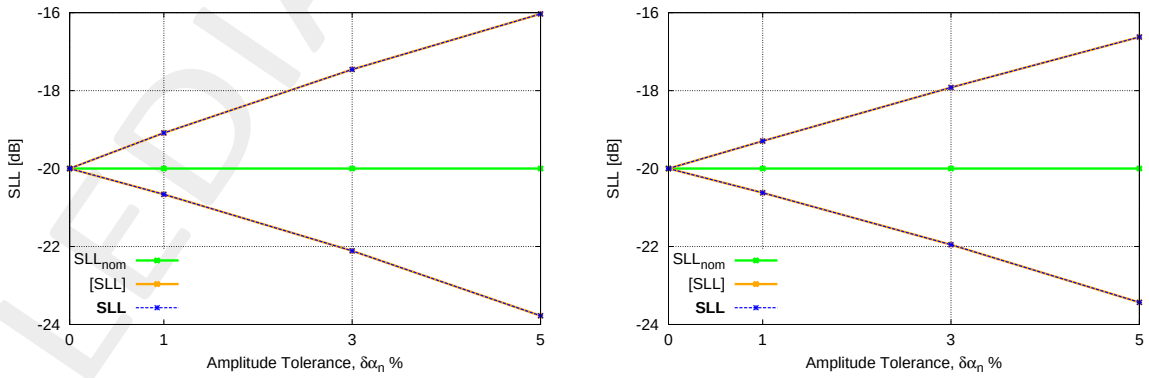

(a) (b)

Figure 32:

Interval Normalized Power Peak vs Amplitude Tolerance

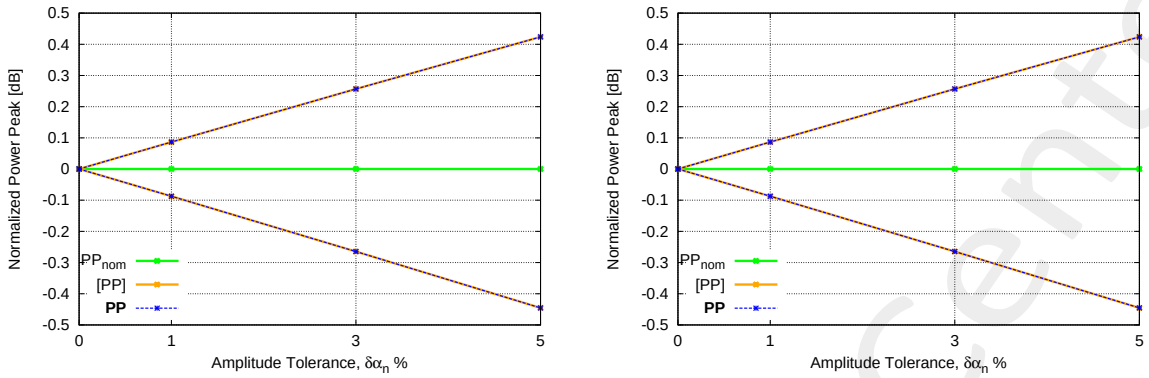

(a) (b)

Figure 33:

Pattern Matching and Normalized Pattern Matching

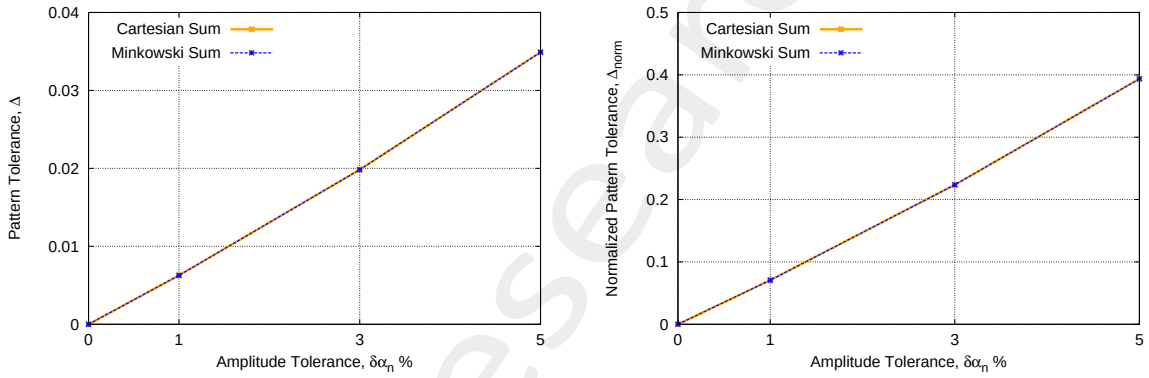

(a) (b)

Figure 34:

Interval Pattern Features - Cuts on the plane $(0,\, v)$ **-** $(u,\, 0)$

Plane $u = 0$

	Cartesian Sum			*Minkowski Sum*		
$\delta\alpha_n\,\%$	$[BW]\ [u]$	$SLL\ [dB]$	$[PP]\ [dB]$	$[BW]\ [u]$	$[SLL]\ [dB]$	$PP\ [dB]$
1	$[0.400,\ 0.422]$	$[-20.66,\ -19.08]$	$[29.20,\ 29.36]$	$[0.400,\ 0.422]$	$[-20.66,\ -19.08]$	$[29.20,\ 29.36]$
3	$[0.376,\ 0.444]$	$[-22.11,\ -17.46]$	$[29.02,\ 29.54]$	$[0.376,\ 0.444]$	$[-22.11,\ -17.46]$	$[29.02,\ 29.54]$
5	$[0.350,\ 0.464]$	$[-23.77,\ -16.03]$	$[28.84,\ 29.70]$	$[0.350,\ 0.464]$	$[-23.77,\ -16.03]$	$[28.84,\ 29.70]$

Table $VIII$:

Plane $v = 0$

	Cartesian Sum			*Minkowski Sum*		
$\delta\alpha_n\,\%$	$[BW]\ [u]$	$SLL\ [dB]$	$[PP]\ [dB]$	$[BW]\ [u]$	$[SLL]\ [dB]$	$PP\ [dB]$
1	[0.190, 0.200]	[−20.62, −19.92]	[29.20, 29.36]	[0.190, 0.200]	[−20.62, −19.92]	[29.20, 29.36]
3	[0.178, 0.210]	[−21.95, −17.92]	[29.02, 29.54]	[0.178, 0.210]	[−21.95, −17.92]	[29.02, 29.54]
5	[0.166, 0.220]	[−23.43, −16.62]	[28.84, 29.70]	[0.166, 0.220]	[−23.43, −16.62]	[28.84, 29.70]

Table IX:

Pattern Matching Δ- Δ_{norm}

	Cartesian Sum		*Minkowski Sum*	
$\delta\alpha_n\,\%$	Δ	Δ_{norm}	Δ	Δ_{norm}
1	6.27×10^{-3}	0.707	6.27×10^{-3}	0.707
3	1.98×10^{-2}	0.224	1.98×10^{-2}	0.224
5	3.59×10^{-2}	0.393	3.59×10^{-2}	0.393

Table X:

1.1.5 Comments and Observations:

The results are the same in both the cases. This is graphical confirmed by the bounds on the pattern and by the interval parameters as well as the values of Δ and Δ_{norm}. As expected, increasing the value of the tolerance on the amplifiers from 1% to 3% and 5% the interval bounds increase.

1.2 10×10 Array Elements

Nominal Pattern

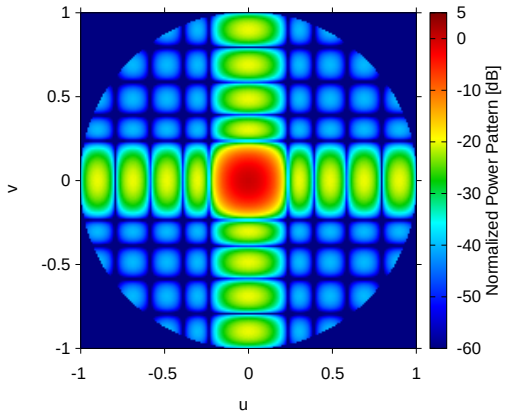

Figure 35:

Nominal Pattern Features

$BW\ [v] - u = 0$	$BW\ [u] - v = 0$	$SLL\ [dB] - u = 0$	$SLL\ [dB] - v = 0$	$PP\ [dB]$
0.196	0.196	-20.0	-20.0	35.84

Table XI:

1.2.1 Amplitude Error 1 %

Interval Pattern

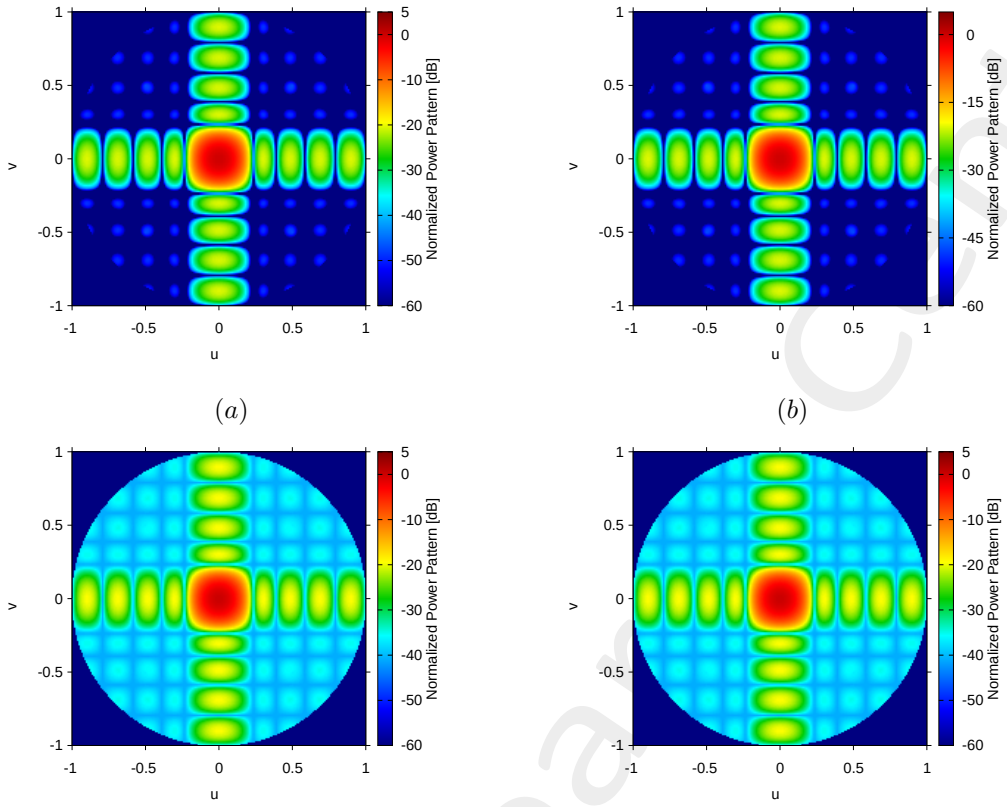

(a) (b)

(c) (d)

Figure 36: Infimum of the power pattern Cartesian (a) and Minkowski sum (b), Supremum of the sum power pattern Cartesian (c) and Minkowski (d) sum

Cuts on the plane $(0, v)$ - $(u, 0)$ - Interval Pattern

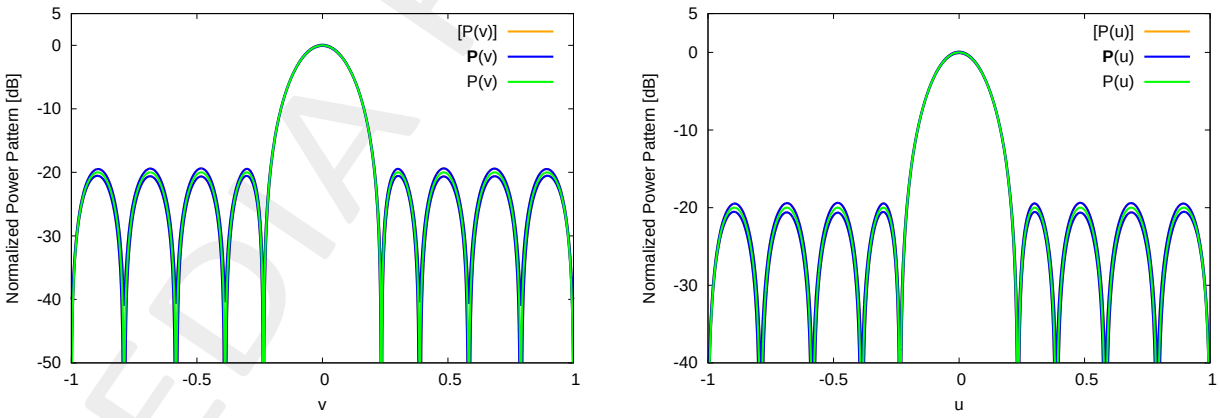

(a) (b)

Figure 37:

1.2.2 Amplitude Error 3 %

Interval Pattern

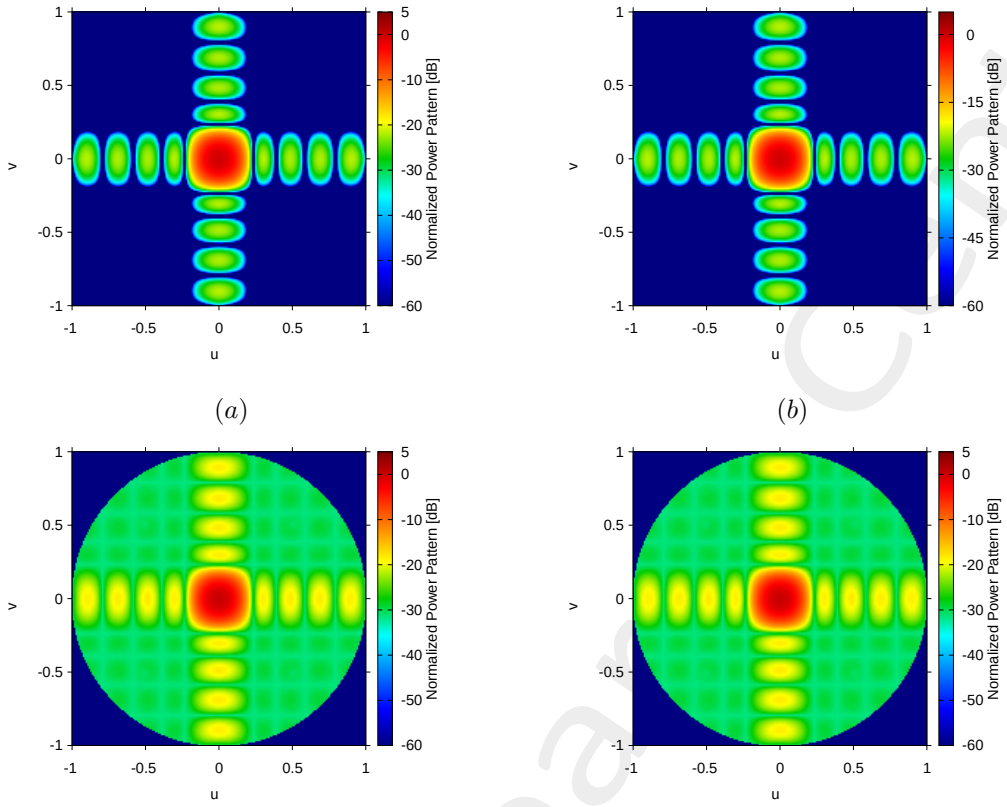

(a) (b)

(c) (d)

Figure 38: Infimum of the power pattern Cartesian (a) and Minkowski sum (b), Supremum of the sum power pattern Cartesian (c) and Minkowski (d) sum

Cuts on the plane $(0, v)$ - $(u, 0)$ - Interval Pattern

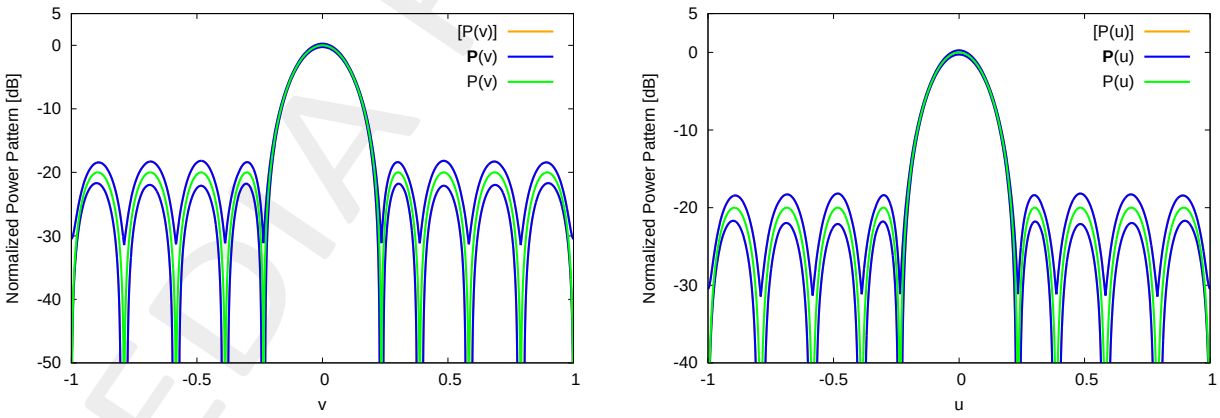

(a) (b)

Figure 39:

1.2.3 Amplitude Error 5 %

Interval Pattern

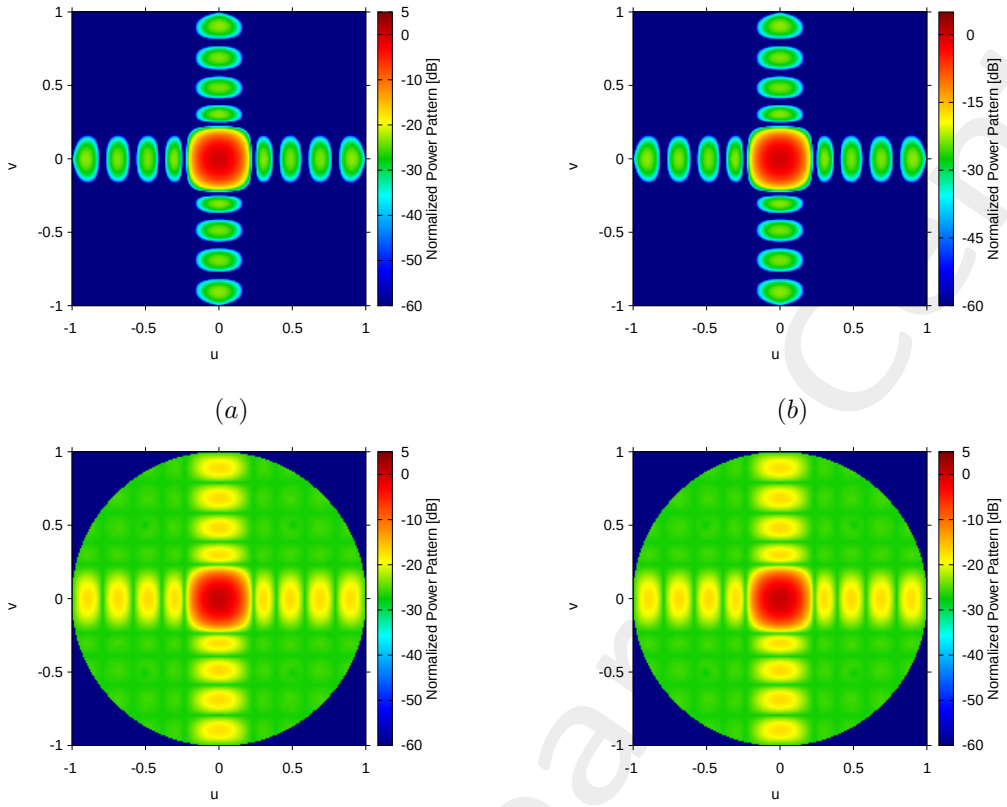

(a) (b)

(c) (d)

Figure 40: Infimum of the power pattern Cartesian (a) and Minkowski sum (b), Supremum of the sum power pattern Cartesian (c) and Minkowski (d) sum

Cuts on the plane $(0, v)$ - $(u, 0)$ - Interval Pattern

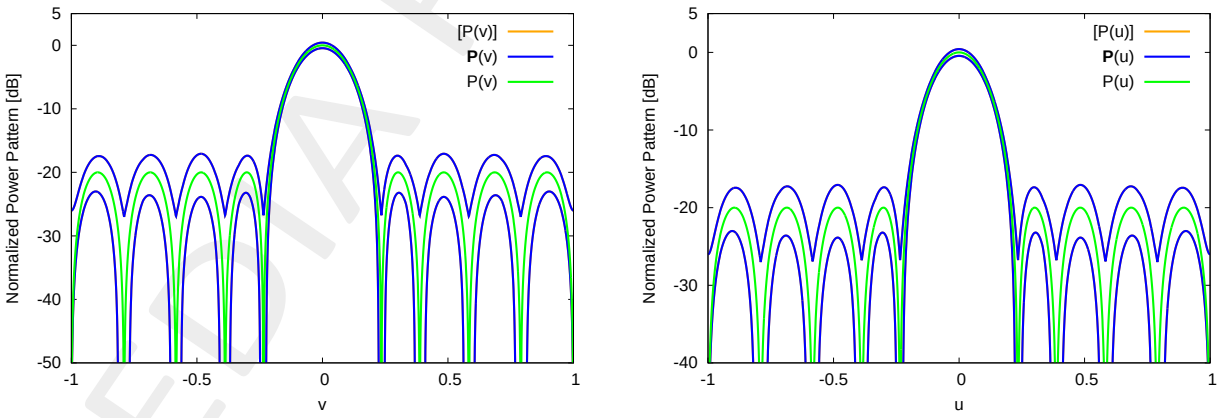

(a) (b)

Figure 41:

1.2.4 Analysis vs Amplitude Tolerance

Pattern

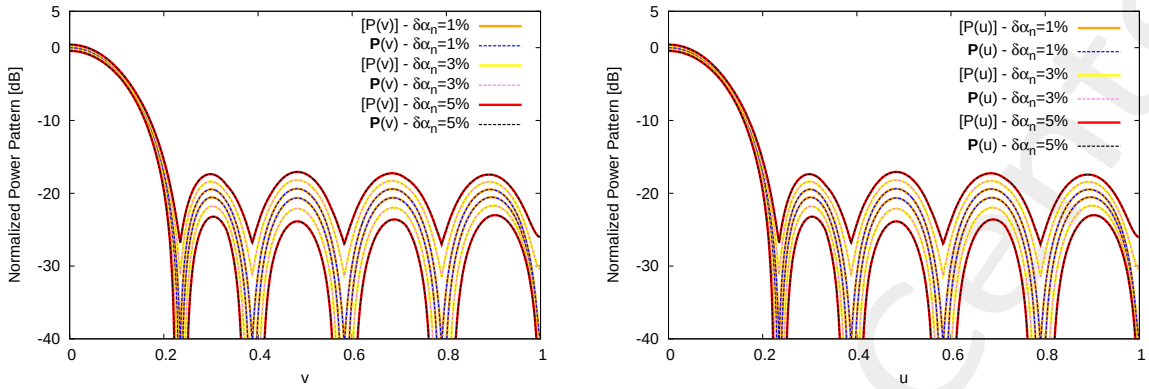

(a) (b)

Figure 42:

Interval Beamwidth

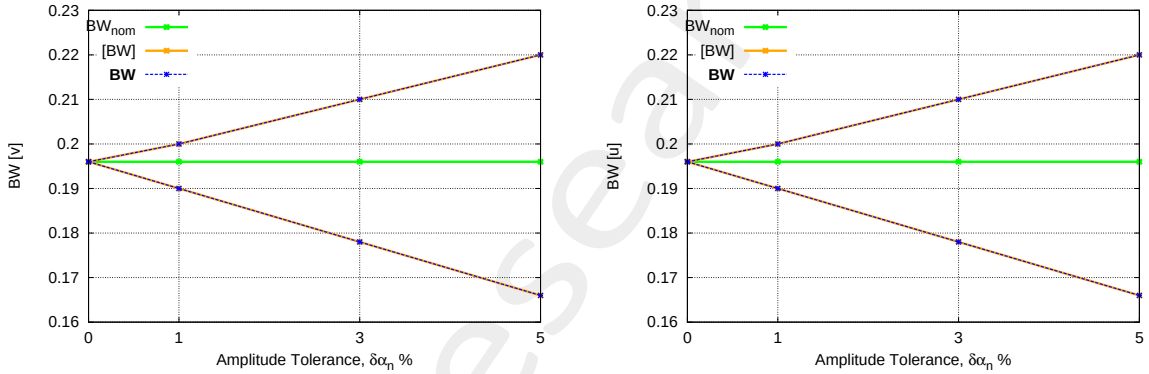

(a) (b)

Figure 43:

Interval SLL

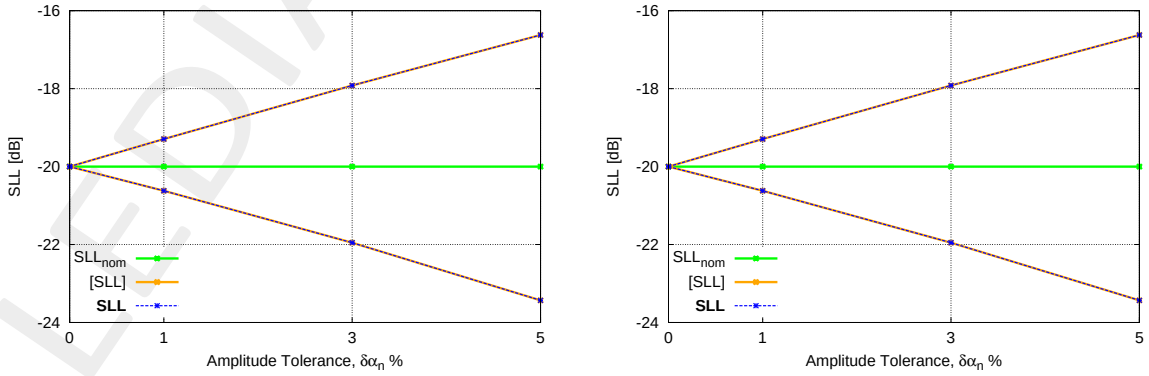

(a) (b)

Figure 44:

Interval Normalized Power Peak vs Amplitude Tolerance

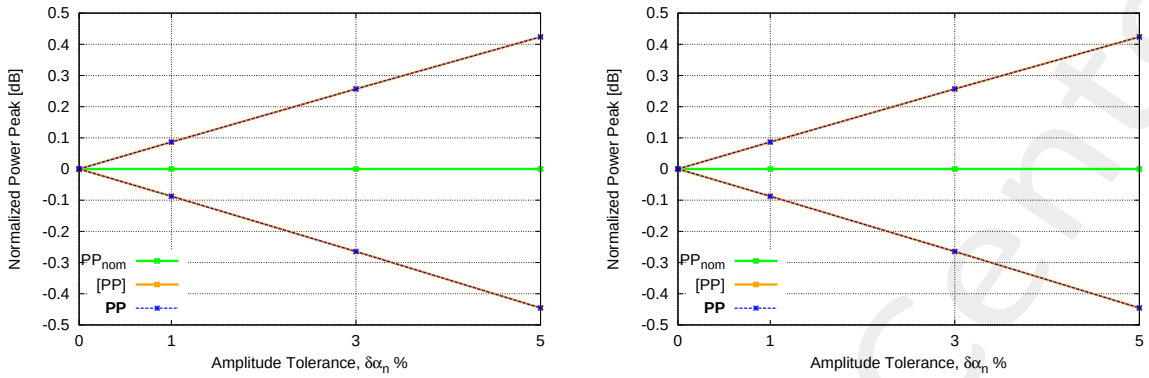

(a) (b)

Figure 45:

Pattern Matching and Normalized Pattern Matching

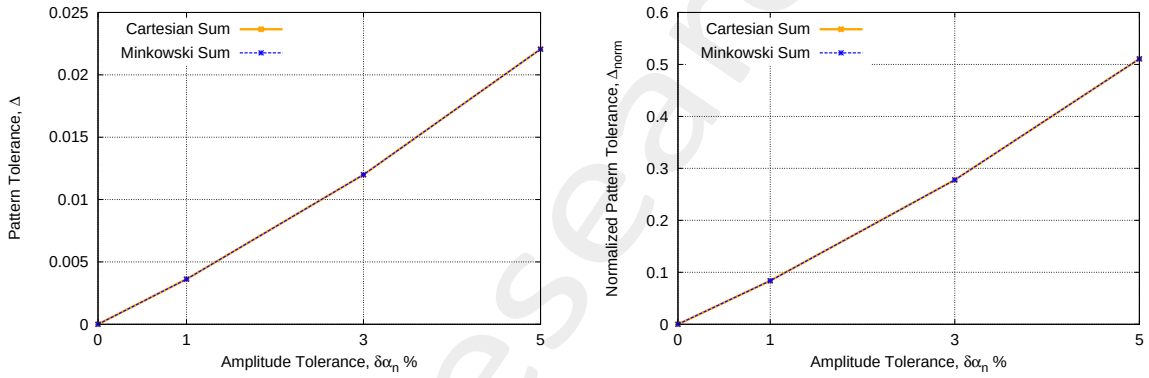

(a) (b)

Figure 46:

Interval Pattern Features - Cuts on the plane $(0,\, v)$ **-** $(u,\, 0)$

Plane $u = 0$

	Cartesian Sum			*Minkowski Sum*		
$\delta\alpha_n$	$[BW]$ $[u]$	SLL $[dB]$	$[PP]$ $[dB]$	$[BW]$ $[u]$	$[SLL]$ $[dB]$	PP $[dB]$
1 %	[0.190, 0.200]	[−20.62, −19.92]	[35.75, 35.93]	[0.190, 0.200]	[−20.62, −19.92]	[35.75, 35.93]
3 %	[0.178, 0.210]	[−21.95, −17.92]	[35.58, 36.10]	[0.178, 0.210]	[−21.95, −17.92]	[35.58, 36.10]
5 %	[0.166, 0.220]	[−23.43, −16.62]	[35.40, 36.27]	[0.166, 0.220]	[−23.43, −16.62]	[35.40, 36.27]

Table XII:

Plane $v = 0$

	Cartesian Sum			*Minkowski Sum*		
$\delta\alpha_n$	$[BW]$ $[u]$	SLL $[dB]$	$[PP]$ $[dB]$	$[BW]$ $[u]$	$[SLL]$ $[dB]$	PP $[dB]$
1 %	[0.190, 0.200]	[−20.62, −19.92]	[35.75, 35.93]	[0.190, 0.200]	[−20.62, −19.92]	[35.75, 35.93]
3 %	[0.178, 0.210]	[−21.95, −17.92]	[35.58, 36.10]	[0.178, 0.210]	[−21.95, −17.92]	[35.58, 36.10]
5 %	[0.166, 0.220]	[−23.43, −16.62]	[35.40, 36.27]	[0.166, 0.220]	[−23.43, −16.62]	[35.40, 36.27]

Table $XIII$:

Pattern Matching Δ- Δ_{norm}

	Cartesian Sum		*Minkowski Sum*	
$\delta\alpha_n$	Δ	Δ_{norm}	Δ	Δ_{norm}
1 %	3.62×10^{-3}	0.083	3.62×10^{-3}	0.083
3 %	1.19×10^{-2}	0.277	1.19×10^{-2}	0.277
5 %	2.20×10^{-2}	0.511	2.20×10^{-2}	0.511

Table XIV:

1.2.5 Comments and Observations:

Also for a bigger planar array, the results are the same in both the cases. This is graphical confirmed by the bounds on the pattern and by the interval parameters as well as the values of Δ and Δ_{norm}. As expected, increasing the value of the tolerance on the amplifiers from 1% to 5% the bounds increase.

References

[1] N. Anselmi, P. Rocca, M. Salucci, and A. Massa, "Optimization of excitation tolerances for robust beamforming in linear arrays," *IET Microw. Antennas Propag.*, vol. 10, no. 2, pp. 208-214, 2016.

[2] P. Rocca, G. Oliveri, R. J. Mailloux, and A. Massa, "Unconventional phased array architectures and design Methodologies - A review," *Proc. IEEE*, vol. 104, no. 3, pp. 544-560, Mar. 2016.

[3] G. Oliveri, M. Salucci, and A. Massa, "Synthesis of modular contiguously clustered linear arrays through a sparseness-regularized solver," *IEEE Trans. Antennas Propag,*, vol. 64, no. 10, pp. 4277-4287, Oct. 2016.

[4] L. Poli, P. Rocca, N. Anselmi, and A. Massa, "Dealing with uncertainties on phase weighting of linear antenna arrays by means of interval-based tolerance analysis," *IEEE Trans. Antennas Propag.*, vol. 63, no. 7, pp. 3299-3234, Jul. 2015.

[5] P. Rocca, N. Anselmi, and A. Massa, "Optimal synthesis of robust beamformer weights exploiting interval analysis and convex optimization," *IEEE Trans. Antennas Propag.*, vol. 62, no. 7, pp. 3603-3612, Jul. 2014.

[6] L. Manica, N. Anselmi, P. Rocca, and A. Massa, "Robust mask-constrained linear array synthesis through an interval-based particle swarm optimisation," *IET Microw. Antennas Propag.*, vol. 7, no. 12, pp. 976-984, Sep. 2013.

[7] N. Anselmi, L. Manica, P. Rocca, and A. Massa, "Tolerance analysis of antenna arrays through interval arithmetic," *IEEE Trans. Antennas Propag.*, vol. 61, no. 11, pp. 5496-5507, Nov. 2013.

[8] P. Rocca, L. Manica, N. Anselmi, and A. Massa, "Analysis of the pattern tolerances in linear arrays with arbitrary amplitude errors," *IEEE Antennas Wireless Propag. Lett.*, vol. 12, pp. 639-642, 2013.

[9] T. Moriyama, L. Poli, N. Anselmi, M. Salucci, and P. Rocca, "Real array pattern tolerances from amplitude excitation errors," *IEICE Electron. Express*, vol. 11, no. 17, pp. 1-8, Sep. 2014.

[10] P. Rocca, N. Anselmi, and A. Massa, "Optimal synthesis of robust array configurations exploiting interval analysis and convex optimization," *IEEE Trans. Antennas Propag.*, vol. 62, no. 7, pp. 3603-3612, Jul. 2014.

[11] N. Anselmi, P. Rocca, M. Salucci, and A. Massa, "Power pattern sensitivity to calibration errors and mutual coupling in linear arrays through circular interval arithmetics," *Sensors*, vol. 16, no. 6 (791), pp. 1-14, 2016.

[12] L. Tenuti, N. Anselmi, P. Rocca, M. Salucci, and A. Massa, "Minkowski sum method for planar arrays sensitivity analysis with uncertain-but-bounded excitation tolerances," *IEEE Trans. Antennas Propag.*, vol. 65, no. 1, pp. 167-177, Jan. 2017.

[13] P. Rocca, N. Anselmi, and A. Massa, "Interval Arithmetic for pattern tolerance analysis of parabolic reflectors," *IEEE Trans. Antennas Propag.*, vol. 62, no. 10, pp. 4952-4960, Oct. 2014.

[14] P. Rocca, L. Poli, N. Anselmi, M. Salucci, and A. Massa, "Predicting antenna pattern degradations in microstrip reflectarrays through interval arithmetic," *IET Microw. Antennas Propag.*, vol. 10, no. 8, pp. 817-826, May 2016.

[15] N. Anselmi, M. Salucci, P. Rocca, and A. Massa, "Generalized sensitivity analysis tool for pattern distortions in reflector antennas with bump-like surface deformations," *IET Microw. Antennas Propag.*, vol. 10, no. 9, p. 909-916, Jun. 2016.